Proceedings of the Korean Nuclear Society Spring Meeting
Cheju. Korea, May 1996

Mechanistic Model of Dryout in a Heat-Generating Porous Medium

Seong Ho Kim
Universitaet Stuttgart, Germany
Soon Heung Chang
Korea Advanced Institute of Science and Technology

Abstract

In the present work the influence of various physical parameters on the two-phase flow behavior in a self-heated porous medium has been studied using a numerical model, that is, the effects of heat generation rate, of porosity, of particle size, and of system pressure on the dryout process. To analyze the effect of these parameters, the variation of both liquid volumetric fraction and liquid axial velocity is evaluated at the steady state or at the onset of a first boiled-out region. The analysis of computational results indicate that a qualitative tendency exists between the parameters such as heat generation rate, porosity, effective particle diameter and the temporal development of the liquid volumetric fraction field up to dryout. In addition to these parameters, a variation of fluid properties such as phase density, phase viscosity due to a change of system pressure can be used for gaining insight into the nature of two-phase flow behavior up to dryout.

1. Introduction

Special attention has been given on the boiling and dryout behavior in a fluid-saturated porous medium composed of heat-generating coarse particles. In the area of safety of light water nuclear reactors, especially, the following system needs to be analyzed for mitigating accident consequences in view of the achievment of long-term cooling of debris particle bed may be formed as one of severe accident sequences: the two-phase flow can be developed when a porous medium fully filled with water is volumetrically heated (e.g., decay heat from nuclear reactor core debris particles or heat released from zirconium oxidation reaction in view of severe accident phenomena). The particle porous medium has an overlying pool of water. The bottom boundary of the medium is both adiabatic and impermeable.

Although, during the boil-off, sufficient water is available via feeding into the medium at the top due to buoyancy, a vapor-liquid countercurrent flow limitation would become a main mechanism that controls the heat removal behavior. Concerning the mitigation of the occurrence of dryout it is certainly interesting to investigate the effect of the main physical parameters on the flow behavior in such a porous body.

The aims of the work are to investigate the influence of various physical parameters on the boiling and dryout behavior in a porous body using a numerical model and to understand qualitative characteristics of dryout phenomena. Physical parameters evaluated in this work are heat generation rate, porosity, particle size, and system pressure. We imply here that the dryout occurs if the liquid volume fraction reduces to zero.

2. Mechanistic Model

In the present work the assumptions used are: incompressible vapor-liquid flow, homogeneous and isotropic particle porous body, temperature-independent thermophysical properties, and thermodynamic equilibrium (i.e., $T_f = T_g = T_s$; $P = P_f = P_g$).

---

* Present address: Korea Advanced Institute of Science and Technology

The continuity equations for liquid and vapor are, respectively

$$\varepsilon \rho_f \frac{\partial}{\partial t}(S_f) + \rho_f \frac{\partial}{\partial z}(U_f) = -\Gamma \ , \tag{1}$$

$$\varepsilon \rho_g \frac{\partial}{\partial t}(S_g) + \rho_g \frac{\partial}{\partial z}(U_g) = \Gamma \ , \tag{2}$$

where ε is the porosity as non-solid volumetric fraction of the system, Γ the vapor generation rate per unit volume, z the axial distance from the bottom of a porous body (negative direction along the gravity). The liquid and vapor volumetric fractions S_f and S_g are related in the non-solid space as

$$S_f + S_g = 1 \ . \tag{3}$$

By extending the empirical Ergun equation for the single-fluid [1], with the aid of the concept of the phase relative permeabilities κ_{rk} and η_{rk} assumed as a function of only the liquid volumetric fraction, the momentum equation for k-phase in a boiling region can be expressed as

$$U_k = - C_{mk0} \cdot \left(\frac{\partial P}{\partial z} + \rho_k \cdot g\right) . \tag{4}$$

The porous flow conductance C_{mk0} can be written

$$C_{mk0} = - \left[\frac{\mu_k}{d_p} \cdot \left(\frac{C_{1k}\, d_p}{\kappa_{rk}} + \frac{C_{2k}\, Re_k}{\eta_{rk}}\right)\right]^{-1} . \tag{5}$$

The first and the second terms on the right hand side of eq. (5) represent the Darcy effect and the Non-Darcy effect, respectively. C_{1k} is the inverse of permeability pertinent to Darcy flow and C_{2k} the inverse of permeability pertinent to Non-Darcy flow for k-phase. The Reynolds number Re_k is

$$Re_k = \frac{\rho_k \, d_p \, |U_k|}{\mu_k} \ . \tag{6}$$

The boundary and initial conditions are

$$P(t, z = H) = P_{sys} \ \text{for all } t > 0 \ , \tag{7}$$

$$U_f(t, z = 0) = 0 \ \text{for all } t > 0 \ , \tag{8}$$

$$U_g(t, z = 0) = 0 \ \text{for all } t > 0 \ , \tag{9}$$

$$S_f(t = 0, z) = 1 \ \text{at } 0 \le z \le H \ . \tag{10}$$

To solve the governing equations for the unknown variables such as P, U_f, U_g, and S_f, the constitutive relationships for Γ, κ_{rk}, η_{rk}, C_{1k}, and C_{2k} must be specified. Under assumptions of the incompressible two-phase flow and the thermodynamic equilibrium for two-phase mixture and solid particle the vapor generation rate Γ can be written as

$$\Gamma = \frac{q'''}{h_{sg} - h_{sf}} \ . \tag{11}$$

The denominator of eq. (11) stands for the latent heat of vaporization of a coolant. The volumetric heat generation rate q''' is chosen as the space-independent quantity. Eq. (11) implies that all of heat generated is used only to change the phase of working fluid.

The relations for the phase relative permeabilities as a function of only the effective liquid volumetric fraction S_f, as proposed in Hofmann and Schulenberg [2], are applied in the work for one-component water-vapor system

$$\kappa_{rk}(S_k) = S_k^{\,3} \ , \tag{12}$$

$$\eta_{rk}(S_k) = S_k^{\,4} \ . \tag{13}$$

C_{1k} and C_{2k} for k-phase are written, respectively, as

$$C_{1k} = E_{1k} \cdot \frac{(1 - \varepsilon)^2}{\varepsilon^3 \, d_p^{\,2}} \ , \tag{14}$$

$$C_{2k} = E_{2k} \cdot \frac{(1 - \varepsilon)}{\varepsilon^3 \, d_p} \ , \tag{15}$$

where E_{1k} and E_{2k} denote the first and the second Ergun constants determined empirically, respectively. Three groups of Ergun constants according to the Reynolds number Re_k, as reported in Fand et al. [3] for single-fluid system, are extended to model the vapor-liquid sytem in the present work.

$$E_{1k} = \begin{cases} 192.24, & 0 < Re_k \le 3 \\ 182, & 3 < Re_k \le 100 \\ 225, & Re_k > 100 \end{cases}, \tag{16}$$

$$E_{2k} = \begin{cases} 0.0, & 0 < Re_k \le 3 \\ 1.92, & 3 < Re_k \le 100 \\ 1.61, & Re_k > 100 \end{cases} \tag{17}$$

In addition, the physical properties μ_k, ρ_k, h_{sk}, and T_s for the coolant, water, are specified using steam tables. Owing to the strong nonlinearity of the coefficients appearing in the governing equations, an iterative four-variable model is used to solve the governing equations numerically.

3. Results

The base case in this work is discussed first with the emphasis on the flow behavior up to dryout in a boiling two-phase region. Then the computational results for other cases are presented to examine the effects of the medium-related parameters such as heat generation rate, porosity, and particle size as well as the fluid-related parameter like system pressure. In the base case, a porous medium with the uniform internal heat generation rate of 3 MW/m^3 was chosen with the medium height of 0.485 m, the porosity of 0.405, and the effective particle diameter of 3.0 mm. The thermophysical properties of water as a working fluid were evaluated at 1 atm system pressure at the top of the medium.

The two-phase flow behavior was studied for the following effects up to dryout in comparison with the base case: the effect of decreasing volumetric heat generation rate, the effect of medium porosity, the effect of effective particle size, and the effect of increasing system pressure at the top. For the effects tested the variation of both liquid volumetric fraction and liquid axial velocity is presented at the steady state or at the onset of a first boiled-out region in Figs. 1 through 8.

Effect of Decreasing Heat Generation Rate on Flow Behavior up to Dryout

The computational results for pure water were presented in Figs. 1 and 2, using various heat generation rate. It is to note that the effect leads physically to that of the decreasing vapor generation rate in a boiling two-phase region. Fig. 1 shows the liquid fraction profiles at the simulation time of incipient dryout. For the cases of 1 MW/m^3 and 2 MW/m^3, the steady state solutions of the liquid fraction existed, but for the base case of 3 MW/m^3 the unsteady flow behavior could only be obtained. Fig. 2 shows the liquid superficial velocity profiles in porous media at the simulation time of incipient dryout.

For a given porous medium with decreasing heat generation rate in comparison with the base case, the rate of change of both the liquid volumetric fraction and the liquid downflowing velocity decreases and arrives earlier at a steady state process. It is shown that the liquid inventory within the medium gets smaller with an increasing heat generation rate as the liquid is more driven out of the medium during the sudden increase in the vapor mass flux.

Effect of Porosity on Flow Behavior up to Dryout

Figs. 3 and 4 show the timewise variation of the liquid volumetric fraction and liquid velocity distributions with respect to the porosity, respectively. For the case of the medium of 0.345 porosity, it was at the height of about 0.40 m at about 36 s that a first boiled-out region occurred, while for the base case (0.405 porosity) at 0.34 m at 42 s. For the case of 0.465 porosity, there was a steady state for two-phase flow.

The effect of increasing porosity of the medium shows that the dryout heat rate required to reach the highest steady state gets higher. It seems that a change in the dryout mechanism within the medium up to dryout occurs as the porosity decreases. The dryout behavior leads to an earlier arrival up to the dryout and a location of dried-out region near the top of a medium.

Effect of Particle Size on Flow Behavior up to Dryout.

Figs. 5 and 6 show the timewise variation of the liquid volumetric fraction and liquid velocity distributions with respect to the particle size, respectively. For the case of the porous body composed of 1.5 mm particle size, it was at the height of about 0.48 m at about 48 s that a first boiled-out region occurred, while for the base case (particle size of 3.0 mm) at 0.34 m at 42 s. For the case of 4.5 mm particle size, there was a steady state for two-phase flow.

For media of large particle size, the liquid volumetric fraction increases with increasing particle diameter and the dryout heat rate gets higher. The dried-out region is later reached and the dryout occurs near the top of a medium as the particle diameter decreases. For the countercurrent system DHF increases with increasing particle size. This seems likely since an increase in particle size causes an increase in permeabilities and less resistance to flow for a given medium [4].

Effect of Increasing System Pressure on Flow Behavior up to Dryout

Figs. 7 and 8 show the temporal variation of the liquid volumetric fraction and liquid velocity distributions with respect to the system pressure, respectively. For the cases of the system pressures of 6.2 bar and 11 bar, there was a steady state for two-phase flow, and the steady liquid volumetric fraction and liquid downflowing velocity were reached, while for the base case (system pressure of 1 atm) it was at the height of about 0.40 m at about 36 s that a first boiled-out region occurred. The more decrease in liquid inventory all over the medium is shown in Fig. 7 as the system pressure is smaller. The slope of negative liquid velocity gradients, as shown in Fig. 8, all over the medium at the steady state region increased with increasing system pressure.

The system pressure has influence on the downflowing liquid mass flux at the steady state as the heat generation rate does. As shown in Fig. 4, therefore, once the heat generation rate and the system pressure are known, the steady state flow behavior in terms of liquid superficial velocity can be predicted. As the system pressure at the top of a medium increases, it seems that the liquid volumetric fraction increases slowly and the more downflowing liquid flows into the medium.

4. Conclusive Remarks

The computational results confirm the qualitative tendency that exists between the medium parameters such as heat generation rate, porosity, effective particle diameter and the temporal development of the liquid volumetric fraction field up to dryout. In addition to the medium parameters, a variation of fluid properties such as phase density, phase viscosity due to a change of reference pressure can be used for gaining insight into the nature of both steady and unsteady flow behavior up to dryout. Furthermore, they emphasize the need of having a good knowledge of the system pressure at the top of a medium as well as of the volumetric heat generation rate inside the medium to predict correctly the transient behavior with the aid of dryout characteristics such as the time required to reach the boiled-out, the axial position of the boiled-out region.

The following might be drawn from the results analyzed:

(1) For a given porous medium with decreasing heat generation rate in comparison with the base case, the rate of change of both the liquid volumetric fraction and the liquid downflowing velocity decreases and arrives earlier at a steady state process.

(2) The effect of increasing porosity of a medium shows that the dryout heat rate required to reach the highest steady state gets higher. The flow behavior leads to an earlier arrival up to the dryout and a location of dried-out region near the top of a medium.

(3) For media of large particle size, the liquid volumetric fraction increases with increasing particle diameter and the dryout heat rate gets higher. The dried-out region is later reached and the dryout occurs near the top of a medium as the particle diameter decreases.
(4) As the system pressure at the top of a medium increases, it seems that the liquid volumetric fraction increases slowly and the more downflowing liquid flows into the medium.

References

[1] S. Ergun, Chem. Eng. Prog. 48 (2), 89-94, 1952.
[2] G. Hofmann and T. Schulenberg, Proc. Int. Meeting on LWR Severe Accidents Evaluation, Cambridge, USA, 18.6-1 - 18.6-8, 1983.
[3] R. M. Fand et al., J. Fluids Eng. 109, 268-274, 1987.
[4] C. Somerton, I. Catton, and L. Thompson, ASME Winter Annual Meeting, 81-WA/HT-17, 1981.

Nomenclature

C_{1k}	inverse of permeability pertinent to Darcy flow (m^{-2})
C_{2k}	inverse of permeability pertinent to Non-Darcy flow (m^{-1})
C_{mk0}	flow conductance of the porous body ($m^3 \cdot s/kg$)
d_p	particle diameter (m)
E_{1k}, E_{2k}	first and second Ergun constants, respectively
g	gravitational constant (m/s^2)
H	height of the porous body (m)
h_{sk}	k-phase specific enthalpy at the saturation condition (J/kg)
P	pressure (Pa)
q'''	volumetric heat generation rate in the porous body (W/m^3)
Re_k	Reynolds number for k-phase
S_k	effective k-phase volumetric fraction
t	time (s)
T	temperature (°C)
U_k	superficial velocity component in the axial coordinate for k-phase (m/s)
z	axial coordinate (m)

Greek

ε	porosity of the porous body
κ_{rk}	relative permeability pertinent to Darcy effect
η_{rk}	relative permeability pertinent to Non-Darcy effect
μ_k	dynamic viscosity for k-phase (Pa·s)
ρ_k	density for k-phase (kg/m^3)
Γ	vapor generation rate per unit volume ($kg/(m^3 \cdot s)$)

Subscripts

f, g, p	liquid, vapor, and solid particle, respectively
k	liquid or vapor
s	saturation conditions
sys	system

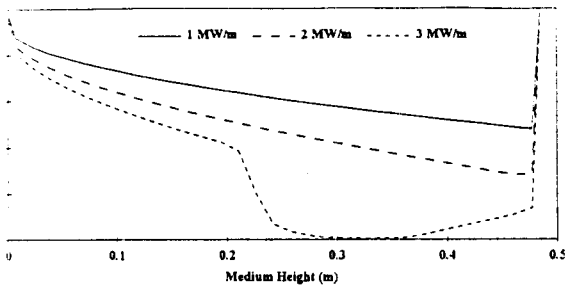

fect of heat generation rate on the axial saturation distribution at t = 43.5 s:
$_{sys}$ = 1 atm, H = 0.485 m, d_p = 3 mm and ε = 0.405 with uniform heat profile.

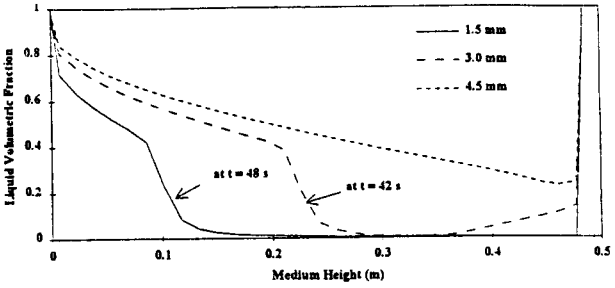

Fig. 5 Effect of particle size on the axial saturation distribution:
P_{sys} = 1 atm, H = 0.485 m, ε = 0.405 and q''' = 3 MW/m^3 with uniform heat profile.

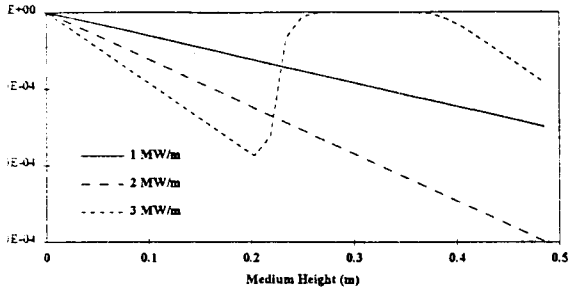

fect of heat generation rate on the axial liquid superficial velocity distribution at t =
.5 s: P_{sys} = 1 atm, H = 0.485 m, d_p = 3 mm and ε = 0.405 with uniform heat profile.

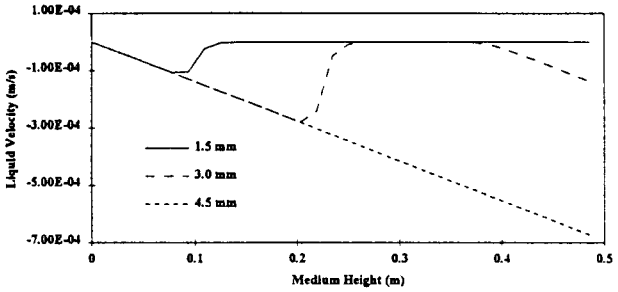

Fig. 6 Effect of particle size on the axial liquid superficial velocity distribution:
P_{sys} = 1 atm, H = 0.485 m, ε = 0.405 and q''' = 3 MW/m^3 with uniform heat profile.

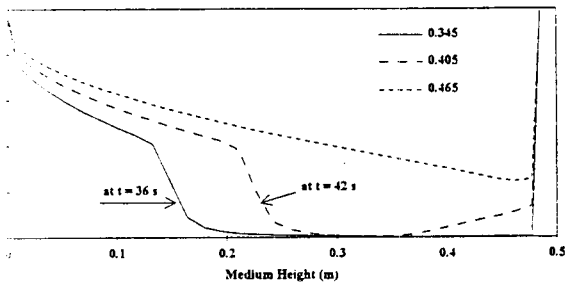

ect of porosity on the axial saturation distribution:
$_s$ = 1 atm, H = 0.485 m, d_p = 3 mm and q''' = 3 MW/m^3 with uniform heat profile.

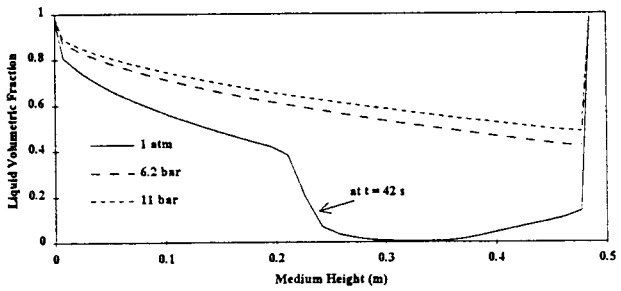

Fig. 7 Effect of system pressure on the axial saturation distribution:
H = 0.485 m, d_p = 3 mm, ε = 0.405 and q''' = 3 MW/m^3 with uniform heat profile.

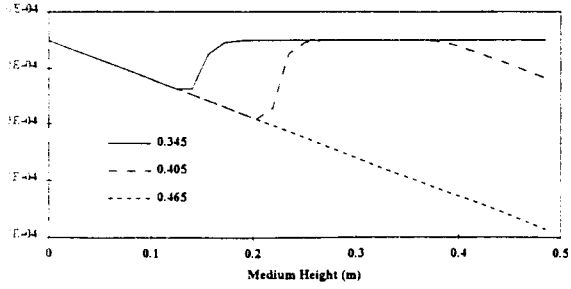

fect of porosity on the axial liquid superficial velocity distribution:
$_s$ = 1 atm, H = 0.485 m, d_p = 3 mm and q''' = 3 MW/m^3 with uniform heat profile.

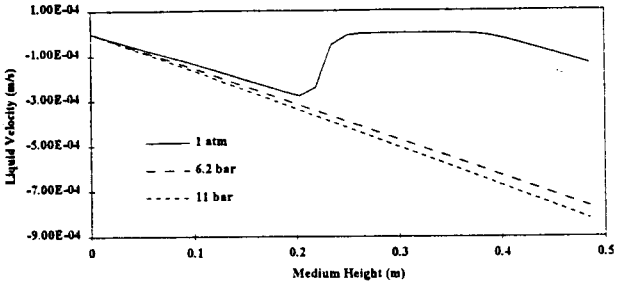

Fig. 8 Effect of system pressure on the axial liquid superficial velocity distribution:
H = 0.485 m, d_p = 3 mm, ε = 0.405 and q''' = 3 MW/m^3 with uniform heat profile.